Hedgehog Signaling in the Drosophila Eye and Head: An Analysis of the Effects of Different *patched Trans*-heterozygotes

Chloe Thomas and Philip W. Ingham[1]

MRC Intercellular Signalling Group, Centre for Developmental Genetics, University of Sheffield, Sheffield S10 2TN, United Kingdom

Manuscript received June 12, 2003
Accepted for publication August 20, 2003

ABSTRACT

Characterization of different alleles of the Hedgehog receptor *patched* (*ptc*) indicates that they can be grouped into several classes. Most mutations result in complete loss of Ptc function. However, missense mutations located within the putative sterol-sensing domain (SSD) or C terminus of *ptc* encode antimorphic proteins that are unable to repress Smo activity and inhibit wild-type Ptc from doing so, but retain the ability to bind and sequester Hh. Analysis of the eye and head phenotypes of *Drosophila melanogaster* in various ptc/ptc^{tuf1} heteroallelic combinations shows that these two classes of *ptc* allele can be easily distinguished by their eye phenotype, but not by their head phenotype. Adult eye size is inversely correlated with head vertex size, suggesting an alteration of cell fate within the eye-antennal disc. A balance between excess cell division and cell death in the mutant eye discs may also contribute to final eye size. In addition, contrary to results reported recently, the role of Hh signaling in the Drosophila head vertex appears to be primarily in patterning rather than in proliferation, with Ptc and Smo having opposing effects on formation of medial structures.

THE Hedgehog (Hh) signaling pathway is necessary for the growth and patterning of many tissue types during the development of both vertebrates and invertebrates (reviewed in McMahon *et al.* 2003). The Hh ligand is received by the transmembrane receptor Patched (Ptc), a negative regulator of the pathway (Ingham *et al.* 1991), which normally inhibits the activity of Smoothened (Smo; Hooper 1994; Alcedo *et al.* 1996). In the presence of Hh, this inhibition is released and the signal is transduced through downstream components, ultimately leading to stabilization and activation of the transcription factor Cubitus interruptus (reviewed in Ingham and McMahon 2001).

Ptc is important not only for repressing Smo, but also for sequestering the Hh protein and thus preventing signaling in inappropriate cells (Chen and Struhl 1996). Ptc is predicted to have two large extracellular loops and 12 transmembrane domains (Nakano *et al.* 1989). The second through sixth of these comprise a putative sterol-sensing domain (SSD), which possesses sequence similarity to those in other proteins such as 3-hydroxy-3-methyl-glutaryl coenzyme A reductase, Niemann-Pick C1, and SREBP cleavage-activating protein (Chin *et al.* 1984; Hua *et al.* 1996; Carstea *et al.* 1997; Loftus *et al.* 1997).

Many alleles corresponding to mutations throughout *ptc* have been isolated, and these can be grouped into three main classes. Gain-of-function alleles are characterized by missense mutations in either of the large extracellular loops and are unable to bind and sequester Hh, resulting in constitutive inhibition of Smo activity (Mullor and Guerrero 2000; Végh and Basler 2003). Antimorphic alleles correspond to missense mutations in the SSD or C terminus of the protein and have the ability to sequester Hh but cannot interact with Smo (Martín *et al.* 2001; Strutt *et al.* 2001). In contrast, the loss-of-function alleles cannot interact with either Hh or Smo and include among them the deletion allele ptc^{G12}, all truncation mutations, and some missense mutations in the extracellular loops. Thus far, analysis of *ptc* alleles has been largely confined to the wing and embryo. However, Hh signaling is required for patterning and growth in many other Drosophila tissues, including the adult eye and head.

The Drosophila compound eye is composed of ~800 ommatidia and develops from the larval eye-antennal imaginal disc (Ready *et al.* 1976). During early third instar, neuronal differentiation occurs in a wave known as the morphogenetic furrow (MF), sweeping from the posterior margin toward the anterior of the eye over a period of ~2 days (Ready *et al.* 1976; Tomlinson 1985, 1988; Tomlinson and Ready 1987). Furrow progression is driven by Hh, which is produced in the developing photoreceptors and moves anteriorly to activate signaling in undifferentiated cells (Heberlein *et al.* 1993; Ma *et al.* 1993).

Hh signaling is known to induce the expression of at least two different signals to mediate photoreceptor

[1]*Corresponding author:* MRC Intercellular Signalling Group, Centre for Developmental Genetics, University of Sheffield, Firth Court, Western Bank, Sheffield S10 2TN, United Kingdom.
E-mail: p.w.ingham@sheffield.ac.uk

differentiation. The long-range TGFβ signaling molecule Decapentaplegic (Dpp) is thought to be responsible for inducing a "preproneural" state in cells ahead of the furrow (Greenwood and Struhl 1999), characterized by the upregulation of proneural repressor genes such as *hairy* (*h*) and *extramacrochaetae* (*emc*), together with cell cycle arrest and synchronization (Horsfield *et al.* 1998). A second signal is believed to act at short range to induce the expression of *atonal* (*ato*), a proneural gene directly required for photoreceptor differentiation (Jarman *et al.* 1994). It is unclear exactly how *ato* is induced, but data implicate the Notch (N) and/or Raf pathways in mediating this process (Greenwood and Struhl 1999; Baonza and Freeman 2001).

In addition to its role in furrow progression, upregulation of Hh at the posterior margin of the eye-antennal disc during early third instar is necessary for the furrow to initiate (Dominguez and Hafen 1997; Borod and Heberlein 1998). Evidence suggests that Hh directly induces the expression of both *dpp* and the gene encoding an eye-specific nuclear protein known as Eyes absent (Eya; Pappu *et al.* 2003). Dpp and Eya interact in a complex manner with a series of other nuclear proteins, including Eyeless (Ey), Eyegone (Eyg), Sine oculis (So), and Dachshund (Dac), to induce furrow initiation (Bonini *et al.* 1997; Chen *et al.* 1997; Pignoni *et al.* 1997; Hazelett *et al.* 1998; Chen *et al.* 1999; Curtiss and Mlodzik 2000). This process is opposed by Wingless (Wg), which inhibits furrow initiation at the anterior of the eye disc (Ma and Moses 1995; Treisman and Rubin 1995). Antagonism between Dpp and Wg plays an earlier role in defining the regions of the disc that correspond to the eye field *vs.* the head vertex (Royet and Finkelstein 1997). In early second instar *wg* is expressed throughout the eye primordium, becoming refined to the presumptive head domain due to Hh-dependent *dpp* expression in the posterior. The patterning of the vertex itself also requires Hh signaling, which is necessary for specification of the medial ocelli and ocellar cuticle, whereas Wg signaling specifies more lateral structures (Royet and Finkelstein 1996). Recent work suggests that Ptc and Smo cooperate to promote cell proliferation in the head, rather than opposing each other as in other tissues (Shyamala and Bhat 2002). According to these authors, loss of either gene causes a reduction in the size of the head capsule, although whether this is due to a loss of Hh-specified medial vertex structures or some other part of the head is unclear.

In addition to its roles in anteroposterior patterning, Hh is also involved in the establishment of the dorsoventral (DV) organizing center, known as the equator, during early second instar (Baker 1978; Campos-Ortega and Waitz 1978). High levels of Hh, Wg, and other unknown molecules, present in the dorsal half of the eye disc, activate the expression of the dorsal selector genes *araucan* (*ara*), *caupolican* (*caup*), and *mirror* (*mirr*), otherwise known as the Iroquois complex (IRO-C; Gomez-Skarmeta *et al.* 1996; McNeill *et al.* 1997; Cavodeassi *et al.* 1999; Lee and Treisman 2001). In turn, IRO-C restricts the production of Fringe (Fng) to the ventral compartment (Cho and Choi 1998; Dominguez and de Celis 1998). Fng is a glycosyltransferase that modulates the ability of cells to respond to Notch ligands (Panin *et al.* 1997; Munro and Freeman 2000). This results in N signaling occurring specifically at the equator where it is essential for growth of the eye disc and upregulation of Hh at the posterior margin prior to furrow initiation (Papayannopoulos *et al.* 1998; Cavodeassi *et al.* 1999).

During analysis of *trans*-heterozygotes carrying the ptc^{tuf1} allele in combination with various alleles of *ptc* (Strutt *et al.* 2001), we noted that the severity of the eye phenotype appeared to be inversely related to that of the wing phenotype. To investigate this phenomenon further, we have studied the eyes and heads of mutant adults in some detail. The eye phenotype differs dramatically between *trans*-heterozygotes carrying loss-of-function and antimorphic *ptc* alleles. However, the head vertex phenotype, while varying in severity between different loss-of-function heteroallelic combinations, is not intrinsically different in those carrying antimorphic alleles. Our results suggest that Hh signaling primarily controls patterning in the head vertex, rather than proliferation as has been recently suggested (Shyamala and Bhat 2002). However, in the presumptive eye, Hh appears to be involved in regulating cell division and cell death in addition to influencing cell fate specification.

MATERIALS AND METHODS

Drosophila stocks: A selection of *ptc* alleles, as described in Strutt *et al.* (2001), was chosen for analysis. ptc^{34}, ptc^{S2}, and ptc^{13} are characterized by missense mutations in the SSD or C terminus of *ptc* and act in an antimorphic way. ptc^{G12}, ptc^{9}, ptc^{14}, ptc^{15}, ptc^{16}, ptc^{17}, ptc^{37}, and ptc^{47} are loss-of-function alleles. The $ptc^{H84lacZ}$ enhancer trap is also a loss-of-function allele. The mild regulatory mutations ptc^{tuf1} (Hidalgo 1989; Capdevila *et al.* 1994) and ptc^{GAL4} (Speicher *et al.* 1994) were also utilized. For analysis of adult phenotypes, controlled crosses were set up in egg-laying cages and embryos were collected on apple-juice/agar plates. To prevent overcrowding, 50 hatched larvae were transferred to each vial of fly food and allowed to mature to adulthood at 25°. For easy analysis of *ptc/*ptc^{tuf1} *trans*-heterozygote larvae, *ptc* alleles were crossed to a *Sco/Cyo,* actGFP line to generate *ptc/Cyo,* actGFP stocks. For analysis of *dpplacZ* expression, a ptc^{tuf1}, *dpplacZ/ Cyo* recombinant line was utilized. A *yw;* $P(w^{+})^{69D}$*D1-12/TM3* (*mirr*$^{B1\text{-}12}$*lacZ*) line was donated by D. Strutt (Choi *et al.* 1996). ptc^{tuf1}*ltd* was crossed to *mirr*$^{B1\text{-}12}$*lacZ* to generate ptc^{tuf1}*ltd, mirr*$^{B1\text{-}12}$*lacZ/Cyo* recombinants. These were then crossed directly to each *ptc* allele for analysis of mutant phenotypes. The hh^{1} allele (Mohler 1988) was donated by D. Strutt. Several *ptc* alleles (ptc^{13}, ptc^{14}, ptc^{16}, ptc^{34}, ptc^{37}, ptc^{47}, and ptc^{tuf1}) were recombined into a hh^{1} background to create *ptc/Cyo*; hh^{1} stocks. ptc^{tuf1}, *dpplacZ/Cyo* was also recombined into the hh^{1} background to create a ptc^{tuf1}, *dpplacZ/Cyo,* hh^{1} stock.

Generation of clones: For making *ptc* clones, *FRT42D,* ptc^{S2}*/ Cyo* and *FRT42D,* ptc^{IIW} *sha/Cyo* were crossed to a *y, hsFLP; FRT42D P(*ry^{+}*,*y^{+}*)/Cyo* line donated by D. Strutt. For making

smo clones, *smo^{D16} Sco, FRT40A/Cyo* and *smo^{Q14}, FRT40A/Cyo* were crossed to a *y, hsFLP; P(y$^+$, hs-CD2)2L-1, FRT40A/Cyo* line donated by D. Strutt. Larvae were heat-shocked at 37° for 2 hr each during early second and early third instar and allowed to develop to adulthood.

Immunohistochemistry: Imaginal discs dissected from 48 hr or late third instar larvae were fixed using standard protocols. Discs were blocked in 1% BSA and incubated overnight at 4° with primary antibodies. After extensive washing, discs were incubated for 2 hr with fluorescent secondary antibodies at room temperature (Jackson Laboratories, West Grove, PA, and Molecular Probes, Eugene, OR). Where necessary, a Cy3-conjugated antiphalloidin or a Cy5-conjugated HRP secondary, donated by D. Strutt, were used to visualize photoreceptors. After further washing, discs were mounted in glycerol and observed with a Leica SP confocal microscope. Primary antibodies were rabbit polyclonal antiatonal (Jarman *et al.* 1994), donated by A. Jarman; mouse monoclonal antiwingless 4D4 (Brook and Cohen 1996); mouse polyclonal antihairy (Carroll and Whyte 1989), donated by K. Howard; rabbit polyclonal anti-phospho-histone-H3 Ser10 from Upstate Biotechnology (Lake Placid, NY; Hendzel *et al.* 1997), donated by P. Rashbass; and rabbit polyclonal anti-β-galactosidase (Cappel). Acridine orange and β-galactosidase staining were carried out using standard protocols. Samples stained with β-galactosidase were observed on a Zeiss Axioplan 2 microscope. All images were manipulated using Photoshop software.

Electron microscopy: Adult eyes were dissected and dehydrated through increasing concentrations of ethanol (25, 50, 75, 90, and 100%), before being critical point dried and mounted on electron microscope specimen-holding stubs. Samples were coated in gold using an Edwards sputter coater and then analyzed on a Phillips PSEM 501B scanning electron microscope.

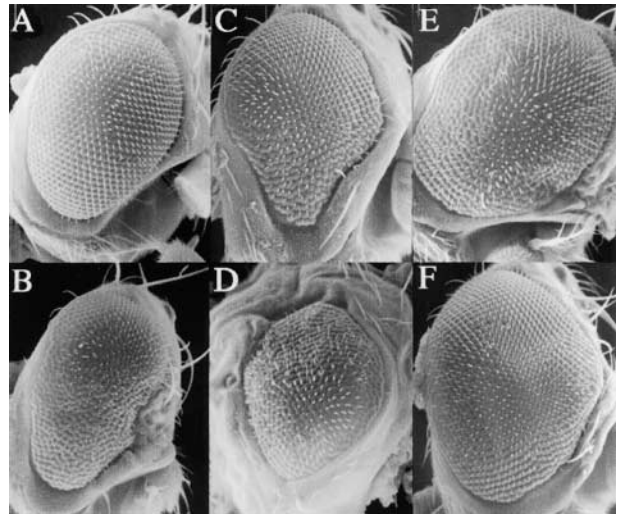

Figure 1.—The adult-eye phenotype of wild type and a selection of *ptc trans*-heterozygous flies shown by scanning electron microscopy. In A–F, anterior is to the left and dorsal is up. (A) The wild-type eye displays an ordered array of ~800 ommatidia and a consistent oval shape. (B–F) All *ptc trans*-heterozygous eyes have a rough appearance: (B) *ptc^{G12}/ptc^{tuf1}*, (C) *ptc^{15}/ptc^{tuf1}*, (D) *ptc^{37}/ptc^{tuf1}*, (E) *ptc^{34}/ptc^{tuf1}*, and (F) *ptc^{S2}/ptc^{tuf1}*. Eyes of mutants carrying loss-of-function *ptc* alleles *in trans* to *ptc^{tuf1}* are generally reduced in size (B–D plus *ptc^{17}/ptc^{tuf1}*, *ptc^{47}/ptc^{tuf1}*, *ptc^{16}/ptc^{tuf1}*, *ptc^{9}/ptc^{tuf1}*, and *ptc^{14}/ptc^{tuf1}*, not shown), while mutants carrying antimorphic *ptc* alleles *in trans* to *ptc^{tuf1}* have enlarged eyes compared to wild type (E and F plus *ptc^{13}/ptc^{tuf1}*, not shown).

RESULTS

Eye phenotype can distinguish between different *ptc* heteroallelic combinations: Lethal *ptc* alleles can be grouped into several classes, including those that have an antimorphic (AN) effect and those that show a loss-of-function (LF) phenotype (Strutt *et al.* 2001). To analyze the role of *ptc* in the development of the Drosophila eye, the phenotypes of adult flies heteroallelic for various *ptc* alleles *in trans* to the *ptc^{tuf1}* allele were observed. *ptc^{tuf1}* is a regulatory mutation that results in a reduced quantity of wild-type protein being produced (Hidalgo 1989; Capdevila *et al.* 1994).

The wild-type eye displays an ordered array of ~800 ommatidia and a consistent oval shape (Figure 1A). The majority of *ptc/ptc^{tuf1}* eyes have disorganized ommatidia leading to a rough appearance (Figure 1, B–F). In addition, most *trans*-heterozygotes show changes in eye shape and size, characteristic of allele class. LF/*ptc^{tuf1}* adults generally have reduced, rounded eyes, although the degree of severity can vary both within and (more strongly) between genotypes. For example, eyes of *trans*-heterozygotes carrying the mild allele *ptc^{15}* (Figure 1C) are almost wild type in appearance, whereas the missense mutation *ptc^{37}* causes an extremely small eye *in trans* to *ptc^{tuf1}* (Figure 1D). The *ptc^{G12}/ptc^{tuf1}* mutant phenotype differs slightly from that of the other LF *trans*-heterozygotes in that the eye is elongated and there appears to be a reduction of surrounding head tissue in some cases (Figure 1B). In contrast, AN/*ptc^{tuf1}* mutants show a marked increase in eye size (Figure 1, E and F), which is consistent within allele class.

Expansion and mispatterning of the head vertex in *ptc trans*-heterozygotes is caused by excess Hh diffusion rather than by ectopic pathway activation: The eye-antennal disc gives rise to the adult eye, antenna, and the head vertex (Haynie and Bryant 1986). As Hh signaling is known to be important in patterning the vertex and, in particular, the ocelli (Royet and Finkelstein 1996), we investigated whether *ptc* mutants cause head defects in an allele-specific manner. In addition to *ptc^{tuf1}*, the *ptc^{GAL4}* allele was analyzed as it has been recently reported that some *ptc^{GAL4} trans*-heterozygous combinations can cause a small head phenotype (Shyamala and Bhat 2002). Like *ptc^{tuf1}*, *ptc^{GAL4}* is homozygous viable, with a mild adult wing and scutellar bristle phenotype due to the insertion of a *P* element containing the *GAL4* gene into the regulatory sequence of *ptc* (Speicher *et al.* 1994).

In wild-type flies, the head vertex is symmetrical and composed of three distinct domains (Figure 2A). The three ocelli are centrally located in the ocellar cuticle, which exhibits a characteristic pattern of bristles. The orbital cuticle is the most lateral region and is also covered in bristles, while the bare-ridged tissue of the frons lies between these two domains.

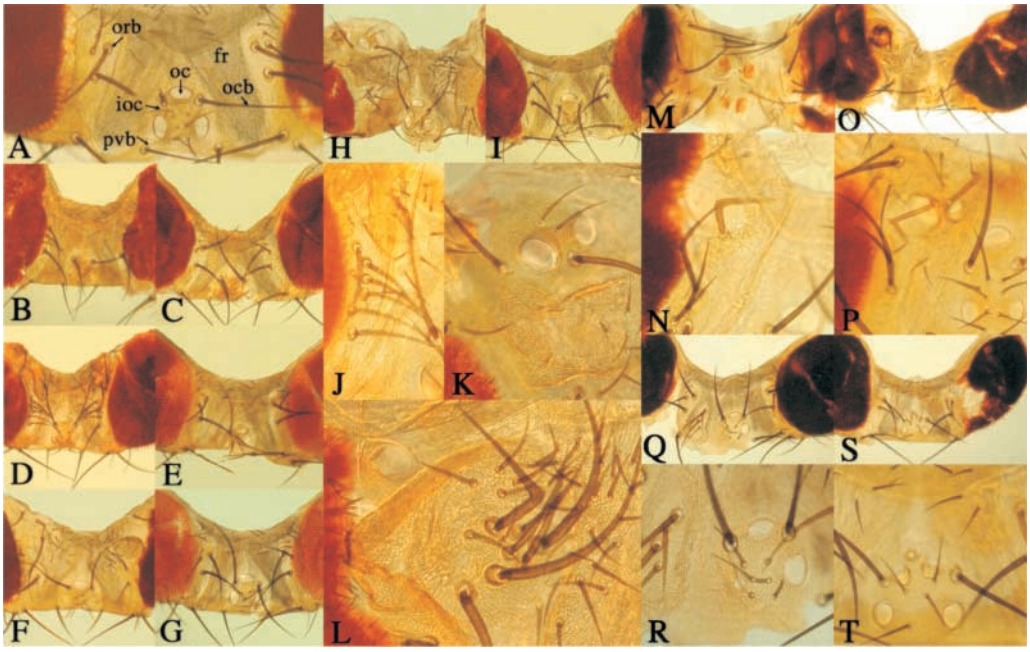

Figure 2.—The consequences of removing *ptc* and *smo* activity in the head vertex. In all panels, anterior is up. (A) Wild-type vertex showing the three ocelli (oc) situated medially in a triangular pattern. Adjacent to these lie the two ocellar bristles (ocb) and the two postvertical bristles (pvb) in addition to several microchaetae known as interocellar bristles (ioc). The frons (fr) is composed of ridged tissue, lateral to the ocellar cuticle. In the most lateral regions lies the orbital cuticle containing three orbital bristles (orb) on each side in addition to microchaetae. (B–L) Head vertex patterning is disrupted in *ptc trans*-heterozygotes. AN *trans*-heterozygotes exhibit a relatively mild head vertex defect: (B) ptc^{34}/ptc^{tuf1}, (C) ptc^{34}/ptc^{GAL4}, (D) ptc^{13}/ptc^{tuf1}, and (E) ptc^{13}/ptc^{GAL4}. LF *trans*-heterozygous heads exhibit a range of severity depending upon the allele: (F) ptc^{G12}/ptc^{tuf1}, (G) ptc^{G12}/ptc^{GAL4}, (H) ptc^{37}/ptc^{tuf1}, and (I) ptc^{37}/ptc^{GAL4}. (J) Magnification of ptc^{13}/ptc^{tuf1} in D, showing ectopic bristles adjacent to eye. (K) Magnification of ptc^{37}/ptc^{tuf1} in S, showing ectopic ocelli. (L) Magnification of ptc^{37}/ptc^{tuf1}, showing an outgrowth of tissue covered in bristles and an ectopic ocellus on the anterior left side of the vertex. (M–T) The consequences of inducing clones in the head vertex lacking *ptc* or *smo* function. Clones are marked with *yellow*, which causes reduced pigmentation of bristles. Due to the limited number of bristles in the head vertex, it is difficult to correctly ascertain clone boundaries. Heads from flies containing clones of (M and N) ptc^{16}, (O and P) ptc^{S2}, (Q and R) smo^{Q14}, and (S and T) smo^{D16} are shown. (M) The medial ocellus is duplicated due to the presence of a clone in the central region. (N) A clone has been magnified, showing an ectopic ocellus adjacent to a *yellow* bristle. (O) An outgrowth of the eye adjacent to an ectopic ocellus indicates a clone spanning the eye and head. In P, another clone has been magnified, showing ectopic ocelli and bristles in the frons. (Q–T) *smo* clones often lack bristles, making it difficult to assess the exact position of the clone using the *yellow* marker. (Q) The left lateral ocellus is almost completely missing (magnified in R); presumably the clone to the left extends into this region. This clone also causes a duplication of the orbital cuticle, presumably due to activation of Hh signaling and hence a more medial fate (frons) on its lateral side. In T, a portion of S has been magnified showing incomplete fusion of the two halves of the medial ocellus.

Mutants were assessed for the overall size and shape of the entire head, in addition to the vertex phenotype (Table 1; Figure 2, A–L). Contrary to the results presented by Shyamala and Bhat (2002), a severely small head phenotype is rarely observed; rather, many heteroallelic combinations show an increase in the size of the vertex (*e.g.*, Figure 2, F and H). This is particularly apparent in mutants with reduced eyes, suggesting a defect in the specification of eye tissue *vs.* head tissue. Some of the ptc^{GAL4} *trans*-heterozygotes, however, do show a slight reduction in head vertex size, although this may not be significant (Table 1). In addition, occasionally one or more antennae are missing, which can give the appearance of a reduced head, particularly in combination with a small-eye phenotype (*e.g.*, ptc^{G12}/ptc^{tuf1}, Figure 2F). It is important to note that there is a variability of at least 5–10% in head vertex size within heteroallelic combinations and even among wild type.

All *trans*-heterozygotes exhibit some degree of mispatterning in the vertex. The most extreme examples possess ectopic ocelli in anterior lateral regions (*e.g.*, Figure 2H, magnified in K)—areas in which eye fate would normally be specified, indicating the activation of high-level Hh signaling. These may be accompanied by outgrowths of tissue, either covered in or devoid of bristles (Figure 2L). AN/ptc^{tuf1} *trans*-heterozygotes do not appear to differ significantly from LF/ptc^{tuf1} with respect to head vertex phenotype. The vertex tends to be closer to wild type in size, with excess bristles in anterior regions and occasionally some ectopic frons or a small outgrowth of tissue (Figure 2, B, D, and J). In this respect the AN alleles behave as mild LF alleles such as ptc^{15} (see Table 1) and do not exhibit an antimorphic phenotype. This suggests that the head defect in the LF/ptc^{tuf1} mutants is caused predominantly by Hh diffusing farther than normal to specify ocellar cuticle fate in competent regions, rather than by ectopic pathway activation (see discussion).

In general, ptc/ptc^{GAL4} *trans*-heterozygotes exhibit milder head, eye, and wing phenotypes than ptc/ptc^{tuf1} combina-

TABLE 1

A summary of head and eye defects in *ptc trans*-heterozygotes

Genotype	Appearance of eye	Head vertex size (% relative to wild type)[a]	% with ectopic ocelli	% with major head defect[b]	% with minor head defect[c]	% missing one or two antennae
13/tuf1	Enlarged	102	0	100	0	0
13/gal4	Wild type	98	0	0	50	0
34/tuf1	Enlarged	117	0	63	37	0
34/gal4	Wild type	94	0	0	9	0
S2/tuf1	Enlarged	125	6	44	56	0
S2/gal4	Wild type	110	0	0	6	0
47/tuf1	Severely reduced	157	56	100	0	33
47/gal4	Mildly reduced	102	0	8	20	4
37/tuf1	Severely reduced	155	50	100	0	27
37/gal4	Mildly reduced	120	2	2	36	0
17/tuf1	Severely reduced	148	2.5	100	0	9
17/gal4	Mildly reduced	122	0	20	13	13
16/tuf1	Severely reduced	140	18	100	0	30
16/gal4	Mildly reduced	105	0	6	6	0
9/tuf1	Severely reduced	146	10	100	0	50
9/gal4	Wild type	108	0	0	29	4
lacz/tuf1	Mildly reduced	145	0	90	10	0
lacz/gal4	Wild type	107	0	0	13	0
G12/tuf1	Severely reduced	136	0	100	0	18
G12/gal4	Wild type	106	0	0	0	0
14/tuf1	Mildly reduced	121	0	0	30	0
14/gal4	Wild type	108	0	0	0	0
15/tuf1	Mildly reduced	117	0	0	30	0
15/gal4	Wild type	105	0	0	3	0
gal4/tuf1	Wild type	99	0	0	5	0

[a] The head vertex area of at least 10 flies of wild type and each *ptc* heteroallelic combination was measured using Improvision Openlab software and then an average was taken for each genotype.

[b] A major head defect is defined as a mutant exhibiting tissue outgrowths, large numbers of ectopic bristles, or many missing bristles.

[c] A minor head defect is defined as a mutant exhibiting one or two missing, extra, or misplaced bristles.

tions do, often appearing almost wild type in both head size and patterning. An exception to this is ptc^{13}/ptc^{GAL4} (Figure 2E), which exhibits ocelli that are larger and closer to one another—a phenotype not observed in any other mutant.

Clones of *ptc* and *smo* cause opposite patterning defects in the head vertex: Shyamala and Bhat (2002) have also reported that clones of cells homozygous for *ptc* or *smo* loss-of-function alleles cause a small head phenotype, implying that both Ptc and Smo act to drive cell proliferation in the head. The results presented above do not support this hypothesis since they indicate that head vertex size is generally increased in mutants with a reduced level of Ptc activity. To investigate this discrepancy further, marked clones of cells expressing various mutant alleles of *ptc* and *smo* were generated (Figure 2, M–T).

In general, *ptc* clones located in medial regions of the head vertex lead to a duplication of macrochaetae and an increase in size of the ocelli, occasionally causing the medial ocellus to be split into two (Figure 2M). In more lateral regions, ectopic ocelli often form, together with ocellar and postvertical bristles (Figure 2, N–P), although if the clone is small then the phenotype is less dramatic. This effect is similar to that caused by clones ectopically expressing *hh* (Royet and Finkelstein 1996) appearing to be slightly milder in the case of ptc^{S2} clones. The presence of ectopic ocelli is often accompanied by an outgrowth in the adjacent eye tissue, suggesting that the clone spans both the eye and head domains (Figure 2O). Very rarely (<1%) there does appear to be a severe reduction in head size if the clone covers the entire vertex (not shown), due to the lack of almost all frons and orbital cuticle.

In contrast, clones lacking wild-type *smo* activity have the most effect when they are located within the ocellar cuticle (Figure 2, Q–T). In this case the ocelli are often smaller in size or even absent. Occasionally the medial ocellus is split into two (Figure 2, S and T), indicating a defect in the fusion of the two half-ocelli during morphogenesis. No obvious change in eye size was noted. Again, infrequently the vertex can be reduced in size if

covered by a large clone. However, the disruption of patterning is conspicuously different from that caused by a *ptc* loss-of-function clone, making it unlikely that Ptc and Smo act in concert to promote growth in the head, as previously suggested (Shyamala and Bhat 2002).

***Trans*-heterozygote eyes are not dorsalized:** In early second instar, the dorsal and ventral compartments of the eye disc and the equator separating them are established. Hh signaling has been implicated in the process of initiating the expression of the Iroquois genes (*caup*, *ara*, and *mirr*), which specify the dorsal compartment (Dominguez and de Celis 1998; Cavodeassi *et al.* 1999). For example, if Hh is ectopically expressed throughout the eye disc using *ey-GAL4*, the IRO-C-expressing dorsal region is expanded and *fng* is restricted to a narrow ventral domain, resulting in a severely reduced, dorsalized eye. This is not dissimilar from the eyes of LF/ptc^{tuf1} mutants, suggesting that excess diffusion of Hh in such *trans*-heterozygotes may cause IRO-C to be activated ectopically in ventral regions.

Investigation of *mirrlacZ* expression (Choi *et al.* 1996) in mutant discs revealed that there is no significant expansion into the ventral region (Figure 3). This is consistent in the adult where red pigment (indicating *mirrlacZ* enhancer trap activity) occupies approximately half the area of the eye (as in the wild type). In some *trans*-heterozygotes, a spot of ectopic *mirr* is present, located at an anterior ventral region (Figure 3, B and C). A notable exception was observed in the ptc^{G12}/ptc^{tuf1} mutants where, very rarely (<2%), the *mirrlacZ* expression is seen to fill the entire eye domain of the disc (Figure 3D). Also occasionally observed in ptc^{G12}/ptc^{tuf1} *trans*-heterozygotes is the induction of an ectopic equator due to ventral expression of *mirr* (Figure 3E), although the eye is still reduced overall when compared with wild type. In general, both classes of mutant display very similar phenotypes, indicating that although correct dorsoventral patterning is clearly perturbed in *ptc trans*-heterozygotes, it does not have a major effect on eye size.

***atonal* expression is reduced in *ptc trans*-heterozygotes:** Atonal acts downstream of Hh in the furrow to initiate the process of neural differentiation (Jarman *et al.* 1994). The exact mechanism of *ato* induction by Hh signaling is still unclear, as at least two independent pathways have been proposed (Greenwood and Struhl 1999; Baonza and Freeman 2001).

In wild-type eye discs, *ato* is initially expressed within the MF in all cell types, but becomes refined into smaller groups of cells and finally is lost in all cells but those destined to become the R8 photoreceptor (Figure 4A; Dokucu *et al.* 1996).

Analysis of the *ptc* mutants indicates that in all allele combinations tested, the overall level of *ato* expression is reduced, but all the stages of resolution of *ato* from a broad stripe to a single cell are still present (Figure 4, B and C).

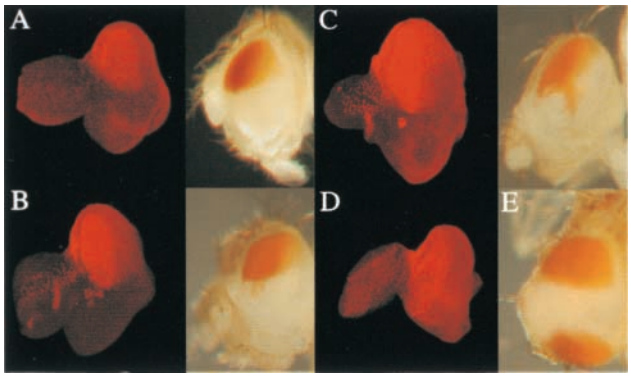

Figure 3.—*ptc trans*-heterozygous eyes are not dorsalized. In all panels, anterior is to the left and dorsal is up. (A) In wild-type larvae, *mirrlacZ* is expressed in the dorsal half of the eye disc, becoming downregulated posterior to the furrow. The *P* element carrying *mirrlacZ* also contains a $white^{+}$ reporter gene, which marks the dorsal compartment of $white^{-}$ adult eyes with red pigment. In *ptc trans*-heterozygotes (B–E), *mirrlacZ* expression is also predominantly confined to the dorsal half of the eye disc, but occasionally ectopic dots of expression are seen in anterior ventral regions. Some adult eyes exhibit a similar spot or extension of pigment into anterior ventral regions, indicating that this tissue has become dorsalized. (B) ptc^{13}/ptc^{tuf1}. Other AN/ptc^{tuf1} *trans*-heterozygotes exhibit a similar phenotype (not shown). (C) ptc^{17}/ptc^{tuf1}. Other LF/ptc^{tuf1} *trans*-heterozygotes generally exhibit a similar phenotype (not shown). (D) Infrequently, *mirrlacZ* expression extends into the ventral compartment of the eye-antennal disc in ptc^{G12}/ptc^{tuf1} *trans*-heterozygotes. (E) Separation of two domains of *mirrlacZ* expression causes an ectopic equator to form in the occasional ptc^{G12}/ptc^{tuf1} mutant. This induces a second morphogenetic furrow, leading to outgrowth of the eye.

***ptc* heteroallelic eye discs show ectopic expression of *dpplacZ*:** Dpp is known to be a direct target of Hh signaling in the eye disc (Heberlein *et al.* 1993; Ma *et al.* 1993) and is therefore a good candidate for a mediator of the effects seen in adult *trans*-heterozygote eyes. Before furrow initiation in wild-type eye discs, *dpp* is expressed in a characteristic horseshoe shape, extending around the lateral and posterior edges of the disc as revealed with a *dpplacZ* reporter (Figure 4D; Blackman *et al.* 1991). Later, the expression refines to a stripe corresponding to the progressing MF and is directly activated by Hh coming from the developing photoreceptors (Figure 4E).

At early third instar, the lateral domains of *dpp* expression are significantly expanded into medial areas of the disc in all *ptc trans*-heterozygous combinations tested (not shown). However, the late expression of *dpp* marking the furrow varies considerably among allele types. In AN/ptc^{tuf1} discs, *dpp* retains a horseshoe appearance due to ectopic "arms" of expression extending anteriorly along the lateral margins before reaching into the center of the disc (Figure 4F). In contrast, LF/ptc^{tuf1} mutants tend to have a thick band of *dpplacZ* expression, of which the posterior edge corresponds to the endogenous *dpp* in the furrow, while the anterior part is ectopic (Figure 4G).

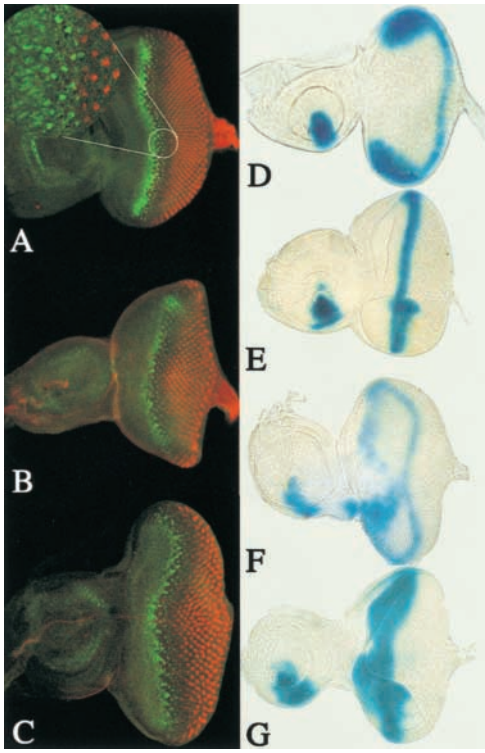

Figure 4.—The expression patterns of Ato and *dpplacZ* are altered in *ptc trans*-heterozygous eye-antennal discs. In all panels, anterior is to the left and dorsal is up. (A–C) Ato expression (green) is counterstained with the neuronal marker HRP in red. (A) In wild-type discs, Ato is first expressed in a stripe of cells at the anterior edge of the furrow and then becomes refined into groups of cells and finally into the single R8 precursor as the furrow passes. In (B) LF or (C) AN *ptc trans*-heterozygotes, the level of Ato staining at all stages appears to be reduced significantly. (B) ptc^{34}/ptc^{tuf1}. (C) AN ptc^{37}/ptc^{tuf1}. Other AN *ptc trans*-heterozygotes exhibit a similar Ato protein expression pattern (not shown). (D–G) In contrast to Ato, *dpplacZ* (blue) is ectopically expressed in *ptc* heteroallelic eye-antennal discs. Before furrow initiation in wild-type discs, *dpplacZ* is expressed in a horseshoe shape (D), later resolving into a stripe that follows the furrow during its progression across the disc (E). AN/ptc^{tuf1} mutants maintain ectopic "arms" of *dpplacZ* expression as the MF progresses. (F) ptc^{34}/ptc^{tuf1}. Other AN/ptc^{tuf1} *trans*-heterozygotes exhibit a similar *dpplacZ* expression pattern (not shown). LF/ptc^{tuf1} mutants exhibit a thickened band of *dpplacZ* expression anterior to the furrow. (G) ptc^{37}/ptc^{tuf1}. Other LF/ptc^{tuf1} *trans*-heterozygotes exhibit a similar *dpplacZ* expression pattern (not shown).

Ectopic Dpp does not give rise to ectopic furrows or cause the eye field to be expanded at the expense of head vertex: Ectopic expression of *dpp* can downregulate *wg* transcription, thus overcoming the inhibitory effects of Wg on MF initiation and allowing the formation of ectopic furrows at the lateral and anterior margins (Chanut and Heberlein 1997; Pignoni and Zipursky 1997). This could lead to overgrowth of the eye tissue and hence to an enlarged eye. However, analysis of furrow and photoreceptor markers (phalloidin and HRP) in the *trans*-heterozygotes suggests that this is not occurring in any allele combination studied (for example, see Figures 4 and 6).

Inhibitory interactions between domains of *wg* and *dpp* expression also define the regions of the disc that become head vertex or eye field, respectively (Figure 5A; Royet and Finkelstein 1997). For example, in the $dpp^{d\text{-}blk}$ mutant, which lacks most Dpp activity in the eye disc (Masucci *et al.* 1990), *wg* expression is expanded and, as a consequence, the eye is severely reduced and replaced with frons cuticle. This suggests that in the converse situation, where *dpp* expression is increased, there may be a downregulation of *wg* and consequently a large eye, small head phenotype. In 48-hr early second instar discs, there is considerable ectopic expression of *dpplacZ* in all *trans*-heterozygotes tested (Figure 5). Wg overlaps *dpplacZ* in the lateral anterior regions, suggesting that it is not transcriptionally downregulated by Dpp, perhaps due to the latter being ectopically expressed at too low a level to have a significant effect. However, the overall domain of *wg* expression does appear slightly reduced in all *ptc* heteroallelic combinations. Since Wg is required for growth of the eye disc (Lee and Treisman 2001; Baonza and Freeman 2002), this could reduce eye size. However, both classes of allele combination show similar *dpplacZ* and Wg staining patterns during second instar (compare Figure 5C with Figure 5D), suggesting that antagonism between Wg and Dpp is not contributing significantly to the final phenotype.

Ectopic Dpp is associated with ectopic expression of the proneural repressor gene *hairy*: Dpp is thought to induce a "preproneural" state in cells anterior to the furrow (Greenwood and Struhl 1999). This is accompanied by the upregulation of genes encoding proneural repressors such as *h*, which repress the expression of *ato* and thus neuronal differentiation (Brown *et al.* 1995; Greenwood and Struhl 1999).

In wild-type eye-antennal discs, H is produced in a broad swath of cells in a domain that is located anterior to the MF (Figure 6A). Double staining for *dpplacZ* indicates that H is expressed in cells immediately abutting those that express *dpp*. In *ptc trans*-heterozygotes, the domain of H expression is expanded anteriorly (Figure 6, B and C), indicating that a greater proportion of cells may be in the preproneural state. In addition, unlike in the wild type, overlap between H and ectopic *dpplacZ* expression is observed (Figure 6C). However, H expression does not reflect the difference in ectopic *dpplacZ* expression observed between the two classes of *ptc trans*-heterozygote, suggesting that if the final eye phenotype is dependent upon ectopic *dpp* expression, this effect is not mediated through H.

Ectopic Dpp is associated with opposing effects on cell division in different regions of the disc: Dpp transcribed in the MF is known to diffuse anteriorly, inducing cell cycle arrest in cells that have previously been dividing asynchronously (Horsfield *et al.* 1998; Green-

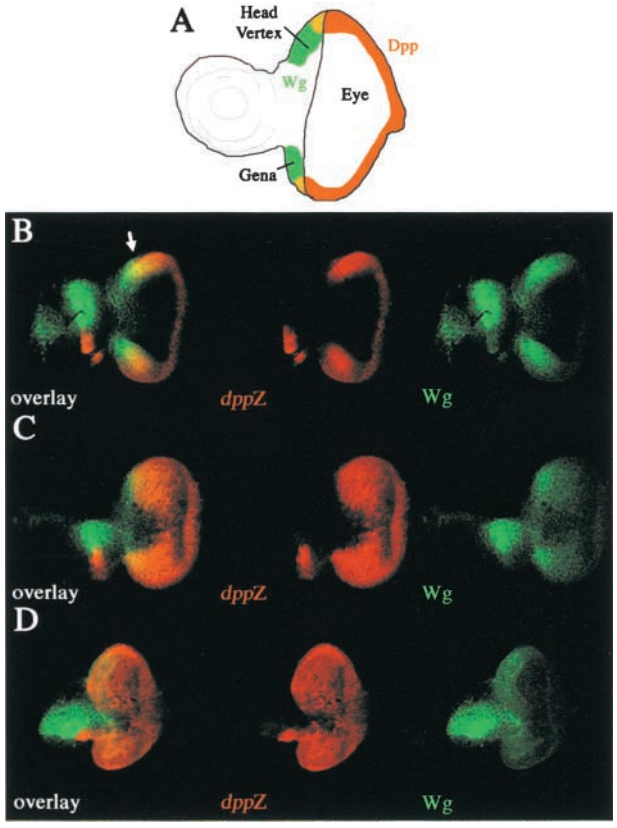

FIGURE 5.—The domain of Wg expression in 48-hr eye-antennal discs is reduced in *ptc trans*-heterozygotes. In all panels anterior is to the left and dorsal is up. (A) A drawing indicating the domains of Wg and Dpp expression in wild-type second instar eye discs and the regions of the disc that are fated to become eye tissue, head vertex, or gena. Overlapping Wg and Dpp expression is indicated in orange. Wg and Dpp are also expressed in the antennal disc (not shown). (B) In wild-type discs, Wg is expressed in the anterior lateral regions of the disc, whereas *dpplacZ* is expressed around the posterior and lateral margins. A small overlap in the expression domains of the two molecules can be observed in the overlay (arrow). (C and D) In *ptc trans*-heterozygotes, Wg staining is reduced and *dpplacZ* is expanded when compared with wild type in both AN/ptc^{tuf1} (C) and LF/ptc^{tuf1} (D) *trans*-heterozygotes as follows: (C) ptc^{13}/ptc^{tuf1} and (D) ptc^{16}/ptc^{tuf1}. Other *ptc trans*-heterozygotes exhibit similar Wg and *dpplacZ* expression patterns (not shown).

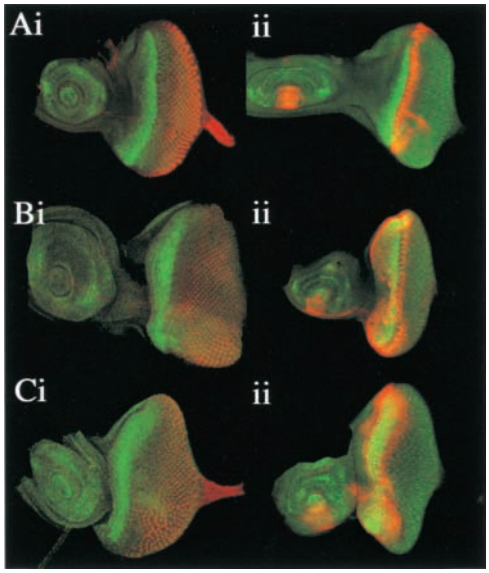

FIGURE 6.—The domain of H expression is expanded in eye-antennal discs ectopically expressing *dpp*. In all panels anterior is to the left and dorsal is up. Discs stained for H expression (green) are counterstained with the neuronal marker HRP (i) or *dpplacZ* (ii) in red. (A) In wild-type discs, H is expressed in a broad stripe of cells anterior to the morphogenetic furrow and the domain of *dpp* expression (ii). The domain of H expression appears to be broader and partially overlaps the domain of ectopic *dpplacZ* expression in both AN/ptc^{tuf1} (B) and LF/ptc^{tuf1} (C) *trans*-heterozygotes. The level of H expression also appears to be slightly weaker than that in wild-type discs. (B) ptc^{34}/ptc^{tuf1}. (C) ptc^{G12}/ptc^{tuf1}. Other *ptc trans*-heterozygotes exhibit a similar H protein expression pattern (not shown).

WOOD and STRUHL 1999). The widened band of *dpp* expression seen ahead of the furrow in LF/ptc^{tuf1} mutant discs could be causing premature cell cycle arrest and hence insufficient growth of the disc. To test this hypothesis, cell division was analyzed using an antibody against phospho-histone H3 (P-H3; HENDZEL *et al.* 1997).

In the wild-type eye disc, a stripe lacking P-H3 expression and corresponding to the cells in the MF that are not dividing is visible (Figure 7A). Posterior to this, nonprecluster cells undergo a synchronous division preceding differentiation (READY *et al.* 1976; WOLFF and READY 1991b), while cell division anterior to the furrow is asynchronous and important for disc growth.

In the mutant discs, the gap in P-H3 expression corresponding to the furrow does not appear to be significantly increased (Figure 7, B and C). Double staining with *dpplacZ* shows that cells are still dividing in areas where ectopic *dpp* is expressed, indicating that Dpp alone is not sufficient to induce cell cycle arrest in such regions. However, the P-H3 staining around the furrow is disorganized compared with wild type: dividing cells anterior and posterior to the furrow are closer together near the equator of the disc than at the poles, suggesting that there may be a deficit in cell division in lateral regions.

Dpp expression prior to furrow initiation and around the margins of the disc is important for proliferation of cells before differentiation (PIGNONI and ZIPURSKY 1997). Compared with wild type, there appears to be an overall increase in cell division ahead of the furrow in the mutants. An average third instar wild-type disc contains 50–70 cells marked with P-H3 ahead of the furrow, compared with 60–120 in *trans*-heterozygote discs. This is particularly apparent in the AN/ptc^{tuf1} *trans*-heterozygotes (90–120 P-H3-positive cells) and thus could partially provide an explanation for the large-eye phenotype. However, the level of ectopic *dpplacZ* around the margins is not obviously greater in AN than in LF

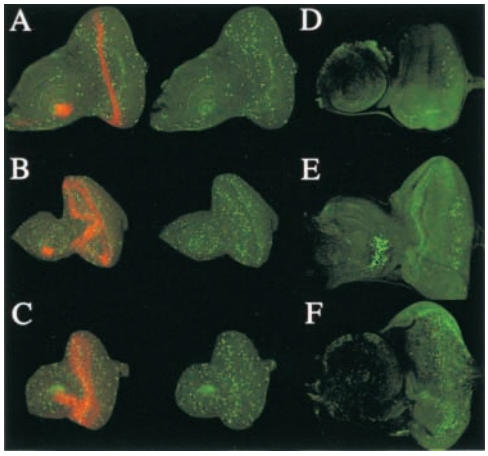

FIGURE 7.—An increase in both cell division and cell death occurs in third instar imaginal discs from *ptc trans*-heterozygotes. Anterior is to the left and dorsal is up. (A–C) Cells in metaphase of mitosis are marked with an antibody against phospho-histone H3 (green). Discs are counterstained with *dpplacZ* (red) in the left-hand panels. (A) In wild-type discs, cells are dividing asynchronously ahead of the furrow. Cell division is absent within the furrow itself, but as it passes, nonprecluster cells undergo a single wave of mitosis to generate the final three photoreceptors and accessory cells. Some cell division is also apparent in the antennal disc. In *ptc* mutant discs, the domain of cell cycle arrest is not significantly wider overall than that seen in wild-type discs. However, its width is uneven along the length of the furrow, being particularly narrow at the equator and wider along the margins, suggesting that less cell division may be occurring in the latter region. (B) ptc^{13}/ptc^{tuf1}. (C) ptc^{37}/ptc^{tuf1}. The numbers of cells undergoing mitosis ahead of the furrow is increased in all mutants, particularly AN/ptc^{tuf1} *trans*-heterozygotes (B), suggesting that this may contribute to the large-eye phenotype seen in such mutants. Cell division also appears to be increased in the antennal region. (D–F) Bright green dots indicate cells undergoing apoptosis, shown by staining with acridine orange. (D) In wild-type discs a small amount of cell death is visible both ahead of the furrow and in several cells behind it (the furrow is visible as a dark line). Cell death posterior to the furrow is significantly increased in all mutants, but may be slightly higher in LF/ptc^{tuf1} *trans*-heterozygotes (E) than in AN/ptc^{tuf1} *trans*-heterozygotes (F). (E) ptc^{13}/ptc^{tuf1}. (F) ptc^{16}/ptc^{tuf1}. Occasionally the level of cell death in the antennal disc is vastly increased (*e.g.*, in E).

trans-heterozygotes, suggesting that other mechanisms are likely to be involved in mediating this difference in cell division.

Mutant eye-antennal imaginal discs show increased levels of cell death behind the furrow: A low level of cell death occurs in wild-type eye discs, both anterior and posterior to the furrow (Figure 7D; WOLFF and READY 1991a). The anterior domain of apoptosis is thought to depend upon the activity of Eya (BONINI *et al.* 1993), but the importance of cell death posterior to the furrow is unknown. In the LF/ptc^{tuf1} *trans*-heterozygotes, apoptosis is increased in a broad swath of cells situated behind the furrow (Figure 7F). Whereas wild-type discs possess <50 cells undergoing apoptosis, LF *trans*-heterozygotes have at least 100 and frequently up to 250 dying cells in this domain. This suggests that abnormally large numbers of differentiated ommatidial cells are dying in the mutants. Surprisingly, AN/ptc^{tuf1} mutant discs also show increased cell death despite the resulting enlarged eye (Figure 7E), although it is not as extensive as in LF/ptc^{tuf1} *trans*-heterozygotes (~100–120 dying cells). Occasionally a vast amount of cell death is seen in the antennal disc (*e.g.*, in Figure 7E), which may correspond to the lack of antennae occasionally seen in some *trans*-heterozygous combinations.

***ptc* heteroallelic combinations can rescue the hh^1 small-eye phenotype:** The homozygous viable hh^1 allele (also known as hh^{bar3}) exhibits a characteristic kidney-shaped eye due to premature furrow arrest. In such discs, *hh* is not expressed in the developing photoreceptor cells and hence cannot drive furrow progression (MOHLER 1988; MOHLER and VANI 1992). Although *dpp* is expressed in lateral regions of the disc, corresponding to the edges of the furrow, it is mainly absent from the furrow itself.

Surprisingly, LF/ptc^{tuf1};hh^1 adult flies have eyes that are closer to wild type in their shape and size than those of either hh^1 or LF/ptc^{tuf1} mutants alone (Figure 8C). The AN/ptc^{tuf1}; hh^1 *trans*-heterozygotes also demonstrate a rescue of hh^1 phenotype, appearing similar to AN/ptc^{tuf1} alone (Figure 8B). This indicates that a reduction in the amount of functional Ptc is sufficient to allow the furrow to progress, even though Hh is not being produced in the photoreceptors. Although ectopic *dpplacZ* is present around the margins in the double mutants, the furrow generally lacks expression, as in the hh^1 single mutant (Figure 8, B and C).

In contrast to *dpplacZ*, *ato* expression is partially rescued in the double mutants. The hh^1 single mutant expresses *ato* early in furrow progression, but loses it in the central regions of the disc during later stages (Figure 8A). Reducing the amount of active Ptc in this situation appears to restore *ato* expression around the equator to a level similar to that seen in *ptc trans*-heterozygous single mutants.

DISCUSSION

Ptc proteins with missense mutations in the SSD or C terminus act as antimorphs in the eye and wing but not in the head: We originally identified antimorphic alleles of *ptc* by the severity of their wing phenotype when heteroallelic with ptc^{tuf1} (STRUTT *et al.* 2001). Such *trans*-heterozygotes exhibit large outgrowths of the anterior wing, consistent with activation of *dpp* due to ectopic Hh signaling, whereas in the hemizygous condition ptc^{tuf1} shows only a mild anterior outgrowth. By contrast, the eye phenotype appears, at least at first sight, to be much more severe in LF/ptc^{tuf1} mutants than in AN/ptc^{tuf1} mutants. However, closer analysis reveals that the two classes of alleles have distinct effects, the eyes of AN/ptc^{tuf1} adults being significantly larger than those of wild type,

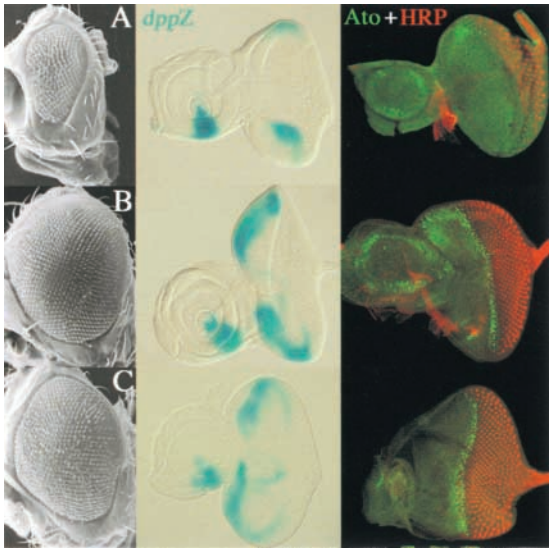

Figure 8.—*Trans*-heterozygous *ptc* mutations rescue the hh^1 adult-eye phenotype, but have less dramatic effects on the expression of different Hh target genes in the eye-antennal disc of hh^1 mutants. Anterior is to the left and dorsal is up. (A) Flies homozygous for the hh^1 allele exhibit narrow kidney-shaped eyes due to premature arrest of the morphogenetic furrow. *dpplacZ* expression is normal at the margins of third instar eye-antennal discs (compare with Figure 6A), but absent in the furrow where it depends directly upon Hh signaling. Ato expression (green) is also absent in the central regions of the disc and becomes downregulated as the furrow arrests. Eye-antennal discs on the right are counterstained with the neuronal marker HRP (red) to visualize developing photoreceptors. (B and C) The hh^1 eye phenotype is rescued when put into a *ptc trans*-heterozygote background. AN/ptc^{tuf1};hh^1 mutants appear similar to those carrying AN/ptc^{tuf1} alone (B), but the LF/ptc^{tuf1} phenotype shows partial rescue with >50% of such flies possessing eyes that are almost wild type in size (C). In double mutants, the expression of *dpplacZ* is not restored in the furrow, although in some cases there does appear to be some residual expression. However, Ato expression does appear to be rescued in the *trans*-heterozygotes, although the domain of expression is generally narrower and less intense than that in wild type (compare with Figure 5A). Mutant genotypes are as follows: (B) ptc^{13}/ptc^{tuf1};hh^1 and (C) ptc^{16}/ptc^{tuf1};hh^1. A similar level of rescue is observed in ptc^{14}/ptc^{tuf1};hh^1, ptc^{34}/ptc^{tuf1};hh^1, ptc^{37}/ptc^{tuf1};hh^1, and ptc^{47}/ptc^{tuf1};hh^1 mutants (not shown).

rather than simply less reduced than those of LF/ptc^{tuf1} mutants. On the other hand, the head defects typical of AN/ptc^{tuf1} *trans*-heterozygotes do appear to be mild versions of those seen in LF/ptc^{tuf1} mutants. Because antimorphic Ptc proteins are distinguished by their ability to sequester the Hh ligand (Johnson *et al.* 2000; Martin *et al.* 2001; Strutt *et al.* 2001), this implies that excessive Hh diffusion, rather than ectopic pathway activation due to Smo derepression, is the principal cause of the head phenotypes such as ectopic ocelli. In summary, it appears that the difference between allele class phenotypes in wing, eye, and head reflects the different relative impact of cell-autonomous ectopic pathway activation *vs.* excess Hh diffusion in the three different structures.

Ptc does not act as a positive regulator of Smo in the head: In the canonical Hh signaling pathway, Ptc functions as a negative regulator (Ingham *et al.* 1991) both by sequestering Hh ligand and by inhibiting Smo activity (Hooper 1994; Alcedo *et al.* 1996; Chen and Struhl 1996). By contrast, Shyamala and Bhat (2002) presented evidence suggesting that Ptc and Smo act in concert to promote growth in the head, a function that is opposed by the activity of Hh. Our reexamination of this issue does not support such an atypical interaction between Ptc and Smo in the head; moreover, it suggests that the predominant role of Hh signaling in the head is in patterning rather than in proliferation.

Although many LF/ptc^{tuf1} mutants have reduced eyes and may lack antennae, there is often a concurrent *increase* in actual head vertex size. Shyamala and Bhat (2002) do not specify whether the reduction in head size they report in ptc^{GAL4} *trans*-heterozygotes is due to a smaller vertex, a reduced eye size, or a lack of antennal structures. However, our results suggest that they are likely observing an effect on the eye and antennae rather than on the head vertex itself, which tends to exhibit only mild bristle defects in such mutants. Their observation that removing one wild-type copy of *smo* in a $ptc^{H84lacZ}$/ptc^{GAL4} background enhances the head defects led them to suggest a novel positive interaction between Ptc and Smo. However, if the reduction in Smo activity results in a decrease in transcription of the mutant *ptc* alleles, phenotypes caused primarily by a lack of Hh sequestration will be enhanced by hemizygosity for *smo*. In *trans*-heterozygotes carrying AN alleles in combination with the ptc^{hdl} allele (generated by Shyamala and Bhat), no head (or wing) defect is apparent (Shyamala and Bhat 2002; our unpublished observations), suggesting that the ability of AN alleles to sequester Hh prevents severe defects from occurring in the head. The lack of wing phenotype also indicates that the Hh pathway is not ectopically activated in this allelic combination, implying that the ptc^{hdl} allele must be able to inhibit Smo quite effectively. If the predominant effect of the ptc^{hdl} mutation is to compromise Hh sequestering activity, this may explain why ptc^{hdl}/LF *trans*-heterozygotes have such severe head defects compared with other LF *trans*-heterozygotes, whereas other tissues that are less sensitive to inefficient Hh sequestration are not affected as strongly in such mutant animals.

We found that generating either *ptc* or *smo* clones in the head vertex resulted in medio-lateral patterning defects. It is difficult to reconcile this with the small head phenotype observed with both *ptc* and *smo* clones by Shyamala and Bhat (2002), particularly as the eyes are often outgrown if they contain *ptc* clones, thus making the head appear larger overall. Inducing particularly large *ptc* or *smo* clones covering the entire vertex does appear to lead to a reduction in head vertex size due to a lack of specification of lateral or medial tissue, respectively. However, this happens extremely rarely and it seems likely that the reduction is due primarily

to the patterning defect and that the resulting lack of proliferation is secondary. In addition, it is documented that both *ptc* and *smo* clones located anteriorly to the anteroposterior boundary of the wing disc, where Hh signaling follows the canonical pathway, can result in similar duplications of anterior wing tissue (Chen and Struhl 1996). This is due to the reduction in *ptc* transcription and hence to Hh sequestration that occurs in both cases, allowing Hh to traverse the clones and ectopically activate signaling at their anterior edge. In conclusion, we find no evidence to suggest that Ptc acts as a positive regulator of Smo in head development.

Expanding the range of Hh activity induces cell death behind the morphogenetic furrow: The eye disc contains two domains of apoptosis: one immediately anterior to the MF that is regulated by Eya and one posterior to the MF whose function is unknown (Wolff and Ready 1991a; Bonini *et al.* 1993). Our findings suggest that the latter domain of cell death is promoted by Hh signaling from photoreceptors. The milder increase in cell death seen in AN/ptc^{tuf1} *trans*-heterozygotes perhaps reflects the efficient sequestration of Hh in such mutants, suggesting that the range of Hh diffusion may be important in influencing the proportion of cells that die behind the MF. Normally, a large amount of cell death, necessary for the elimination of two to three excess pigment cells per ommatidium, occurs in pupal eye discs (Wolff and Ready 1991a). Cell death behind the MF may have a similar function, perhaps in removing cells mis-specified during differentiation. It is possible that Hh could regulate apoptosis through activation of a molecule at short range behind the MF. Alternatively, cell death may not depend directly upon Hh, but rather upon the presence of increased numbers of mis-specified cells in *ptc* mutants that may result in cell death occurring to regulate differentiation effectively.

The consequences of increased Hh signaling in the eye: The earliest known role of Hh in the eye imaginal disc is to help specify the dorso-ventral organizer (Cavodeassi *et al.* 1999). Incorrect DV specification compromises the function of N in promoting growth, resulting in small eyes (Papayannopoulos *et al.* 1998). However, the small-eye phenotype seen in LF/ptc^{tuf1} appears to be unconnected to this process. Although some disorganization of the equator is seen in *ptc trans*-heterozygotes, it is not significant, and its presence in both classes of mutant indicates that the effect, if any, on eye size is small.

The two major targets of Hh signaling during MF progression are *dpp* and *ato* (Heberlein *et al.* 1993; Ma *et al.* 1993; Jarman *et al.* 1994). Our data indicate that although *dpp* is ectopically activated in *ptc trans*-heterozygotes, *ato* is not. This is unexpected as Hh signaling activates the initial expression of *ato* (Jarman *et al.* 1994), so an increase might be anticipated to expand the *ato* expression domain into more anterior regions, while maintaining or even increasing the level of expression. Conversely, reducing the activity of *ptc* in the hh^{1} mutant rescues the expression of *ato*, but not that of *dpp*. There are several possible explanations for these findings. First, *ato* is an indirect target of Hh signaling and the mediators of Hh activity in this context are unclear. It is likely that other factors, in addition to those directly induced by Hh, are necessary for *ato* expression, any one of which may be limiting. Second, *dpp* may respond to lower levels of Hh pathway activation more than genes upstream of *ato*. In the wing disc, *dpp* is activated by relatively low levels of Hh anterior to the AP border (Ingham and Fietz 1995; Zecca *et al.* 1995), whereas other Hh target genes such as *collier* require a higher level of pathway activation (Vervoort *et al.* 1999). In *ptc trans*-heterozygotes some Ptc activity is retained and hence the very highest level of Hh signaling cannot be reached. Third, Dpp in its role as an inducer of the preproneural state can actually inhibit the expression of *ato* through activation of the proneural repressors *h* and *emc* (Greenwood and Struhl 1999). In *ptc trans*-heterozygous discs, the domain of *h* expression does appear to be expanded, suggesting a possible explanation for the observed downregulation of *ato* expression. A fourth possibility that has not been tested is that the increased level of Hh signaling in *ptc trans*-heterozygote discs results in an expansion of the domain of *rough* (*ro*) expression. Ro is induced by high-level Hh signaling at the posterior margin of the MF (Dominguez 1999), but, if expressed at excessive levels (as in the ro^{Dom} mutant), causes a downregulation of *ato* expression (Chanut *et al.* 2000). Although a severe reduction in *ato* expression such as that caused by ro^{Dom} can result in furrow arrest, the significance of a mild downregulation of expression is unknown.

The two classes of mutants both show an increase in *dpplacZ* expression relative to wild type. However, the domain of ectopic expression differs significantly between allele types, suggesting a difference in the way in which the pathway is activated in the two classes of mutant. Because LF *ptc* alleles cannot sequester Hh efficiently (Strutt *et al.* 2001), the broad band of ectopic *dpplacZ* seen ahead of the MF may be caused by excessive diffusion of Hh anteriorly. In contrast, the AN/ptc^{tuf1} *trans*-heterozygotes can sequester Hh efficiently and consequently demonstrate only phenotypes caused by autonomous ectopic pathway activation.

Despite the rescue of adult-eye phenotype observed in ptc/ptc^{tuf1};hh^{1} double mutants, the expression of *dpplacZ* was not restored in the center of the disc. Since Dpp does not play a major role in MF progression (Burke and Basler 1996; Greenwood and Struhl 1999), the lack of expression in this situation may not have a significant effect. Alternatively, excessive *dpp* expression at the margins may allow the protein to diffuse medially into the disc, thus aiding MF progression in an unconventional way.

Dpp is known to have several functions in the eye disc, all of which, when modified, can influence the final size and shape of the adult eye. However, despite

the disparity between the patterns of *dpplacZ* expression in the two types of *trans*-heterozygote, surprisingly little difference is detected downstream of Dpp. Although ectopic *dpp* expression has been shown to induce ectopic MFs (Chanut and Heberlein 1997; Pignoni and Zipursky 1997), this does not occur in the *ptc trans*-heterozygotes, presumably because the ectopic Dpp is either not high enough or not expressed in the right place.

In addition to its effect on furrow initiation, Dpp is also responsible for defining the eye field via inhibition of Wg and for inducing cell cycle arrest ahead of the furrow (Royet and Finkelstein 1997; Horsfield *et al.* 1998). Small-eye mutants do show an increased head vertex size, suggesting that an eye-to-vertex fate change has occurred. However, *ptc trans*-heterozygotes do not display critical differences either from wild type or between allele classes in the distribution of Wg in second instar eye discs. In addition, *dpp* expression is actually expanded in eye discs of small-eye mutants, indicating that processes other than Wg/Dpp antagonism must be involved in specification of eye *vs.* head domains.

Ectopic Dpp ahead of the furrow does not appear to induce premature cell cycle arrest and therefore cannot explain the reduced-eye phenotypes observed in LF/ptc^{tuf} *trans*-heterozygotes. However, when compared to wild type, *ptc* mutants do show an increase in cell divisions ahead of the furrow. We suggest that in addition to an eye/head vertex specification defect, LF/ptc^{tuf1} *trans*-heterozygotes may exhibit a small-eye phenotype due to excessive cell death, despite some increase in cell divisions ahead of the furrow. Conversely, in DN/ptc^{tuf1} *trans*-heterozygotes, increased proliferation could overcompensate for increased cell death, leading to larger eyes. This suggests that the adult-eye phenotype is at least partially dependent upon a balance between cell division and cell death in the disc, in addition to an eye-to-head fate change.

We thank David Strutt, Andrew Jarman, Ken Howard, and Penny Rashbass for antibodies and/or Drosophila stocks. We are also grateful to Monica Kibart for maintenance of Drosophila stocks and John Proctor for assisting with scanning electron microscopy. The confocal microscopy facility at the Centre for Developmental Genetics is funded by a grant from Yorkshire Cancer Research. This analysis was supported by a Wellcome Trust Program grant to P.W.I.

LITERATURE CITED

Alcedo, J., M. Ayzenzon, T. Von Ohlen, M. Noll and J. E. Hooper, 1996 The Drosophila *smoothened* gene encodes a seven-pass membrane protein, a putative receptor for the Hedgehog signal. Cell **86:** 221–232.

Baker, W. K., 1978 A clonal analysis reveals early developmental restrictions in the Drosophila head. Dev. Biol. **62:** 422–463.

Baonza, A., and M. Freeman, 2001 Notch signalling and the initiation of neural development in the Drosophila eye. Development **128:** 3889–3898.

Baonza, A., and M. Freeman, 2002 Control of Drosophila eye specification by Wingless signalling. Development **129:** 5313–5322.

Blackman, R. K., M. Sanicola, L. A. Raftery, T. Gillevet and W. M. Gelbart, 1991 An extensive 3′ *cis*-regulatory region directs the imaginal disk expression of *decapentaplegic*, a member of the TGF-β family in Drosophila. Development **111:** 657–665.

Bonini, N. M., W. M. Leiserson and S. Benzer, 1993 The *eyes absent* gene: genetic control of cell survival and differentiation in the developing Drosophila eye. Cell **72:** 379–395.

Bonini, N. M., Q. T. Bui, G. L. Gray-Board and J. M. Warrick, 1997 The Drosophila *eyes absent* gene directs ectopic eye formation in a pathway conserved between flies and vertebrates. Development **124:** 4819–4826.

Borod, E. R., and U. Heberlein, 1998 Mutual regulation of *decapentaplegic* and *hedgehog* during the initiation of differentiation in the Drosophila retina. Dev. Biol. **197:** 187–197.

Brook, W. J., and S. M. Cohen, 1996 Antagonistic interactions between Wingless and Decapentaplegic responsible for dorsal-ventral pattern in the Drosophila leg. Science **273:** 1373–1377.

Brown, N. L., C. A. Sattler, S. W. Paddock and S. B. Carroll, 1995 Hairy and Emc negatively regulate morphogenetic furrow progression in the Drosophila eye. Cell **80:** 879–887.

Burke, R., and K. Basler, 1996 Hedgehog-dependent patterning in the Drosophila eye can occur in the absence of Dpp signaling. Dev. Biol. **179:** 360–368.

Campos-Ortega, J. A., and M. Waitz, 1978 Cell clones and pattern formation: developmental restrictions in the compound eye of Drosophila. Wihelm Roux's Arch. Dev. Biol. **184:** 155–170.

Capdevila, J., M. P. Estrada, E. Sanchez-Herrero and I. Guerrero, 1994 The Drosophila segment polarity gene *patched* interacts with *decapentaplegic* in wing development. EMBO J. **13:** 71–82.

Carroll, S. B., and J. S. Whyte, 1989 The role of the *hairy* gene during Drosophila morphogenesis: stripes in imaginal discs. Genes Dev. **3:** 905–916.

Carstea, E. D., J. A. Morris, K. G. Coleman, S. K. Loftus, D. Zhang *et al.*, 1997 Niemann-Pick C1 disease gene: homology to mediators of cholesterol homeostasis. Science **277:** 228–231.

Cavodeassi, F., R. Diez Del Corral, S. Campuzano and M. Dominguez, 1999 Compartments and organising boundaries in the Drosophila eye: the role of the homeodomain Iroquois proteins. Development **126:** 4933–4942.

Chanut, F., and U. Heberlein, 1997 Role of *decapentaplegic* in initiation and progression of the morphogenetic furrow in the developing Drosophila retina. Development **124:** 559–567.

Chanut, F., A. Luk and U. Heberlein, 2000 A screen for dominant modifiers of ro(Dom), a mutation that disrupts morphogenetic furrow progression in Drosophila, identifies *groucho* and *hairless* as regulators of atonal expression. Genetics **156:** 1203–1217.

Chen, R., M. Amoui, Z. Zhang and G. Mardon, 1997 Dachshund and Eyes absent proteins form a complex and function synergistically to induce ectopic eye development in Drosophila. Cell **91:** 893–903.

Chen, R., G. Halder, Z. Zhang and G. Mardon, 1999 Signaling by the TGF-β homolog *decapentaplegic* functions reiteratively within the network of genes controlling retinal cell fate determination in Drosophila. Development **126:** 935–943.

Chen, Y., and G. Struhl, 1996 Dual roles for Patched in sequestering and transducing Hedgehog. Cell **87:** 553–563.

Chin, D. J., G. Gil, D. W. Russell, L. Liscum, K. L. Luskey *et al.*, 1984 Nucleotide sequence of a 3-hydroxy-3-methyl-glutaryl coenzyme A reductase, a glycoprotein of endoplasmic reticulum. Nature **308:** 613–617.

Cho, K., and K. W. Choi, 1998 Fringe is essential for mirror symmetry and morphogenesis in the Drosophila eye. Nature **396:** 272–276.

Choi, K. W., B. Mozer and S. Benzer, 1996 Independent determination of symmetry and polarity in the Drosophila eye. Proc. Natl. Acad. Sci. USA **93:** 5737–5741.

Curtiss, J., and M. Mlodzik, 2000 Morphogenetic furrow initiation and progression during eye development in Drosophila: the roles of *decapentaplegic*, *hedgehog* and *eyes absent*. Development **127:** 1325–1336.

Dokucu, M. E., S. L. Zipursky and R. L. Cagan, 1996 Atonal, Rough and the resolution of proneural clusters in the developing Drosophila retina. Development **122:** 4139–4147.

Dominguez, M., 1999 Dual role for Hedgehog in the regulation of the proneural gene *atonal* during ommatidia development. Development **126:** 2345–2353.

Dominguez, M., and J. F. de Celis, 1998 A dorsal/ventral boundary established by Notch controls growth and polarity in the Drosophila eye. Nature **396:** 276–278.

Dominguez, M., and E. Hafen, 1997 Hedgehog directly controls initiation and propagation of retinal differentiation in the Drosophila eye. Genes Dev. **11:** 3254–3264.

Gomez-Skarmeta, J., R. Diez Del Corral, E. De La Calle-Mustiennes, D. Ferres-Marco and J. Modolell, 1996 *araucan* and *caupolican*, two members of the novel Iroquois complex, encode homeoproteins that control proneural and vein-forming genes. Cell **85:** 95–105.

Greenwood, S., and G. Struhl, 1999 Progression of the morphogenetic furrow in the *Drosophila* eye: the roles of Hedgehog, Decapentaplegic and the Raf pathway. Development **126:** 5795–5808.

Haynie, J. L., and P. J. Bryant, 1986 Development of the eye-antenna imaginal disc and morphogenesis of the adult head in *Drosophila melanogaster*. J. Exp. Zool. **237:** 293–308.

Hazelett, D. J., M. Bourouis, U. Walldorf and J. E. Treisman, 1998 *decapentaplegic* and *wingless* are regulated by *eyes absent* and *eyegone* and interact to direct the pattern of retinal differentiation in the eye disc. Development **125:** 3741–3751.

Heberlein, U., T. Wolff and G. M. Rubin, 1993 The TGFß homolog *dpp* and the segment polarity gene *hedgehog* are required for propagation of a morphogenetic wave in the Drosophila retina. Cell **75:** 913–926.

Hendzel, M. J., Y. Wei, M. A. Mancini, A. Van Hooser, T. Ranalli *et al.*, 1997 Mitosis-specific phosphorylation of histone H3 initiates primarily within pericentric heterochromatin during G2 and spreads in an ordered fashion coincident with mitotic chromosome condensation. Chromasoma **106:** 348–360.

Hidalgo, A., 1989 Molecular cloning of *ptc* and analysis of its role in intrasegmental patterning in *D. melanogaster*. Ph.D. Thesis, University of Oxford, Oxford.

Hooper, J. E., 1994 Distinct pathways for autocrine and paracrine Wingless signalling in Drosophila embryos. Nature **372:** 461–464.

Horsfield, J., A. Penton, J. Secombe, M. Hoffman and H. Richardson, 1998 *decapentaplegic* is required for arrest in G_1 phase during Drosophila eye development. Development **125:** 5069–5078.

Hua, X., A. Nohturfft, J. L. Goldstein and M. S. Brown, 1996 Sterol resistance in CHO cells traced to point mutation in SREBP cleavage-activating protein. Cell **87:** 415–426.

Ingham, P. W., and M. J. Fietz, 1995 Quantitative effects of Hedgehog and Decapentaplegic activity of the patterning of the *Drosophila* wing. Curr. Biol. **5:** 432–440.

Ingham, P. W., and A. P. McMahon, 2001 Hedgehog signalling in animal development: paradigms and principles. Genes Dev. **15:** 3059–3087.

Ingham, P. W., A. M. Taylor and Y. Nakano, 1991 Role of the Drosophila *patched* gene in positional signalling. Nature **353:** 184–187.

Jarman, A. P., E. H. Grell, L. Ackerman, L. Y. Jan and Y. N. Jan, 1994 *atonal* is the proneural gene for Drosophila photoreceptors. Nature **369:** 398–400.

Johnson, R. L., L. Milenkovic and M. P. Scott, 2000 In vivo functions of the Patched protein: requirement of the C-terminus for target gene inactivation but not Hedgehog sequestration. Mol. Cell **6:** 467–478.

Lee, J. D., and J. E. Treisman, 2001 The role of Wingless signaling in establishing the anteroposterior and dorsoventral axes of the eye disc. Development **128:** 1519–1529.

Loftus, S. K., J. A. Morris, E. D. Carstea, J. D. Gu, C. Cummings *et al.*, 1997 Murine model of Niemann-Pick C disease: mutation in a cholesterol homeostasis gene. Science **277:** 232–235.

Ma, C., and K. Moses, 1995 *wingless* and *patched* are negative regulators of the morphogenetic furrow and can affect tissue polarity in the developing Drosophila compound eye. Development **121:** 2279–2289.

Ma, C., Y. Zhou, P. A. Beachy and K. Moses, 1993 The segment polarity gene *hedgehog* is required for progression of the morphogenetic furrow in the developing Drosophila eye. Cell **75:** 927–938.

Martin, V., G. Carrillo, C. Torroja and I. Guerrero, 2001 The sterol-sensing domain of Patched protein seems to control Smoothened activity through Patched vesicular trafficking. Curr. Biol. **11:** 601–607.

Masucci, J. D., R. J. Miltenberger and F. M. Hoffmann, 1990 Pattern-specific expression of the Drosophila *decapentaplegic* gene in imaginal disks is regulated by 3′ *cis*-regulatory elements. Genes Dev. **4:** 2011–2023.

McMahon, A. P., P. W. Ingham and C. J. Tabin, 2003 Developmental roles and clinical significance of Hedgehog signaling. Curr. Top. Dev. Biol. **53:** 1–114.

McNeill, H., C. H. Yang, M. Brodsky, J. Ungos and M. A. Simon, 1997 *mirror* encodes a novel PBX-class homeoprotein that functions in the definition of the dorsal-ventral border in the Drosophila eye. Genes Dev. **11:** 1073–1082.

Mohler, J., 1988 Requirements for *hedgehog*, a segmental polarity gene, in patterning larval and adult cuticle of Drosophila. Genetics **120:** 1061–1072.

Mohler, J., and K. Vani, 1992 Molecular organisation and embryonic expression of the *hedgehog* gene involved in cell-cell communication in segmental patterning in Drosophila. Development **115:** 957–971.

Mullor, J. L., and I. Guerrero, 2000 A gain-of-function mutant of *patched* dissects different responses to the Hedgehog gradient. Dev. Biol. **228:** 211–224.

Munro, S., and M. Freeman, 2000 The Notch signalling regulator Fringe acts in the Golgi apparatus and requires the glycosylransferase signature motif DXD. Curr. Biol. **10:** 813–820.

Nakano, Y., I. Guerrero, A. Hidalgo, A. Taylor, J. R. S. Whittle *et al.*, 1989 A protein with several possible membrane-spanning domains encoded by the Drosophila segment polarity *patched*. Nature **341:** 508–513.

Panin, V. M., V. Papayannopoulos, R. Wilson and K. D. Irvine, 1997 Fringe modulates Notch-ligand interactions. Nature **387:** 908–912.

Papayannopoulos, V., A. Tomlinson, V. M. Panin, C. Rauskolb and K. D. Irvine, 1998 Dorsal-ventral signaling in the Drosophila eye. Science **281:** 2031–2034.

Pappu, K. S., R. Chen, B. W. Middlebrooks, C. Woo, U. Heberlein *et al.*, 2003 Mechanism of *hedgehog* signaling during Drosophila eye development. Development **130:** 3053–3062.

Pignoni, F., and S. L. Zipursky, 1997 Induction of Drosophila eye development by Decapentaplegic. Development **124:** 271–278.

Pignoni, F., B. Hu, K. H. Zavitz, J. Xiao, P. A. Garrity *et al.*, 1997 The eye-specification proteins So and Eya form a complex and regulate multiple steps in Drosophila eye development. Cell **91:** 881–891.

Ready, D. F., T. E. Hanson and S. Benzer, 1976 Development of the Drosophila retina, a neurocrystalline lattice. Dev. Biol. **53:** 217–240.

Royet, J., and R. Finkelstein, 1996 *hedgehog*, *wingless* and *orthodenticle* specify adult head development in Drosophila. Development **122:** 1849–1858.

Royet, J., and R. Finkelstein, 1997 Establishing primordia in the Drosophila eye-antennal disc: the roles of *decapentaplegic*, *wingless* and *hedgehog*. Development **124:** 4793–4800.

Shyamala, B. V., and K. M. Bhat, 2002 A positive role for Patched-Smoothened signaling in promoting cell proliferation during normal head development in Drosophila. Development **129:** 1839–1847.

Speicher, S. A., U. Thomas, U. Hinz and E. Knust, 1994 The *serrate* locus of Drosophila and its role in morphogenesis of the wing imaginal discs: control of cell proliferation. Development **120:** 535–544.

Strutt, H., C. Thomas, Y. Nakano, D. Stark, B. Neave *et al.*, 2001 Mutations in the sterol-sensing domain of Patched suggest a role for vesicular trafficking in Smoothened regulation. Curr. Biol. **11:** 608–613.

Tomlinson, A., 1985 The cellular dynamics of pattern formation in the eye of Drosophila. J. Embryol. Exp. Morphol. **89:** 313–331.

Tomlinson, A., 1988 Cellular interactions in the developing Drosophila eye. Development **104:** 183–193.

Tomlinson, A., and D. F. Ready, 1987 Neuronal differentiation in the Drosophila ommatidium. Dev. Biol. **120:** 366–376.

Treisman, J. E., and G. M. Rubin, 1995 *wingless* inhibits morphogenetic furrow movement in the Drosophila eye disc. Development **121:** 3519–3527.

Végh, M., and K. Basler, 2003 A genetic screen for Hedgehog targets involved in the maintenance of the Drosophila anteroposterior compartment boundary. Genetics **163:** 1427–1438.

Vervoort, M., M. Crozatier, D. Valle and A. Vincent, 1999 The COE transcription factor Collier is a mediator of short-range Hedgehog-induced patterning of the Drosophila wing. Curr. Biol. **9:** 632–639.

Wolff, T., and D. F. Ready, 1991a Cell death in normal and rough eye mutants of Drosophila. Development **113:** 825–839.

Wolff, T., and D. F. Ready, 1991b The beginning of pattern formation in the Drosophila compound eye: the morphogenetic furrow and the second mitotic wave. Development **113:** 841–850.

Zecca, M., K. Basler and G. Struhl, 1995 Sequential organizing activities of engrailed, hedgehog and decapentaplegic in the *Drosophila* wing. Development **121:** 2265–2278.

Communicating editor: K. Anderson